Molecular Biology of the Cell
Vol. 15, 3285–3295, July 2004

Excessive Myosin Activity in *Mbs* Mutants Causes Photoreceptor Movement Out of the *Drosophila* Eye Disc Epithelium

Arnold Lee and Jessica E. Treisman*

Skirball Institute for Biomolecular Medicine and Department of Cell Biology, New York University School of Medicine, New York, New York 10016

Submitted January 21, 2004; Revised March 15, 2004; Accepted March 29, 2004
Monitoring Editor: Anne Ridley

Neuronal cells must extend a motile growth cone while maintaining the cell body in its original position. In migrating cells, myosin contraction provides the driving force that pulls the rear of the cell toward the leading edge. We have characterized the function of myosin light chain phosphatase, which down-regulates myosin activity, in *Drosophila* photoreceptor neurons. Mutations in the gene encoding the myosin binding subunit of this enzyme cause photoreceptors to drop out of the eye disc epithelium and move toward and through the optic stalk. We show that this phenotype is due to excessive phosphorylation of the myosin regulatory light chain Spaghetti squash rather than another potential substrate, Moesin, and that it requires the nonmuscle myosin II heavy chain Zipper. *Myosin binding subunit* mutant cells continue to express apical epithelial markers and do not undergo ectopic apical constriction. In addition, mutant cells in the wing disc remain within the epithelium and differentiate abnormal wing hairs. We suggest that excessive myosin activity in photoreceptor neurons may pull the cell bodies toward the growth cones in a process resembling normal cell migration.

INTRODUCTION

The cytoskeleton plays a variety of roles during development, allowing cells to change their shape, adhesive properties, and motility (Jamora and Fuchs, 2002). Two critical components of the cytoskeleton are actin and nonmuscle myosin II. The contractile activity of actomyosin complexes has been implicated in cell migration, epithelial sheet movements, cytokinesis, axon outgrowth, and cell adhesion (Maciver, 1996; Jacinto *et al*., 2002; Dent and Gertler, 2003). During migration of several cell types, myosin activity is required to retract the rear of the cell (Ridley *et al*., 2003).

Nonmuscle myosin II consists of a hexamer of two myosin heavy chains (MHC), two myosin light chains (MLC), and two myosin regulatory light chains (MRLC) (Korn and Hammer, 1988). Phosphorylation of key serine and threonine residues on MRLC stimulates the ATPase activity of MHC and promotes its assembly into filaments, leading to stress fiber contraction (Adelstein and Conti, 1975; Craig *et al*., 1983; Umemoto *et al*., 1989; Katoh *et al*., 2001). Mutations in the *Drosophila* orthologs of these myosin subunits have provided insight into the developmental functions of myosin II. Mutations in *zipper* (*zip*), which encodes MHC, cause defects in cytokinesis, closure of the dorsal embryonic epidermis over the amnioserosa, axon patterning, and myofibril formation (Zhao *et al*., 1988; Young *et al*., 1993; Bloor and Kiehart, 2001). *spaghetti squash* (*sqh*), encoding MRLC, is required for cytokinesis, oogenesis, and imaginal disc eversion (Karess *et al*., 1991; Wheatley *et al*., 1995; Edwards and Kiehart, 1996; Jordan and Karess, 1997).

Actin-binding proteins of the ezrin, radixin, and moesin (ERM) family are thought to link transmembrane proteins to the actin cytoskeleton (Bretscher, 1999). ERM proteins are activated by phosphorylation of a conserved threonine residue, which inhibits association between the N-terminal FERM domain and C-terminal actin-binding domain of the protein, freeing them to bind to other substrates (Matsui *et al*., 1998; Pearson *et al*., 2000). Moesin-like (Moe) is the only representative of this family in *Drosophila*. *Moe* mutants have abnormal oocyte polarity because defects in the anchorage of actin filaments to the oocyte cortex disrupt the localization of maternal determinants (Jankovics *et al*., 2002; Polesello *et al*., 2002). In addition, *Moe* mutant cells in the wing disc undergo an epithelial-to-mesenchymal transition and adopt invasive migratory behavior (Speck *et al*., 2003).

Interestingly, genetic and biochemical studies implicate the same kinase and phosphatase in the regulation of both nonmuscle myosin II and Moesin. Rho-associated kinase (ROCK/Rok) has been shown to phosphorylate MRLC in both mammalian and *Drosophila* systems (Amano *et al*., 1996; Mizuno *et al*., 1999; Winter *et al*., 2001). Myosin light chain kinase (MLCK) also can phosphorylate and activate MRLC; MLCK seems to act at the periphery of the cell, whereas ROCK is active in more central regions (Bresnick, 1999; Totsukawa *et al*., 2000). Although ERM proteins are positively regulated by Rho GTPases, it is not clear whether they are directly phosphorylated by ROCK or by phosphoinositide-regulated kinases (Fukata *et al*., 1998; Matsui *et al*., 1998, 1999). However, in *Drosophila* wing disc development *Moe* seems to act antagonistically to *Rho1* and *rok* (Speck *et al*., 2003).

A major antagonist of the Rok/myosin signaling pathway is myosin light chain phosphatase (MLCP). This serine/

Article published online ahead of print. Mol. Biol. Cell 10.1091/mbc.E04–01–0057. Article and publication date are available at www.molbiolcell.org/cgi/doi/10.1091/mbc.E04–01–0057.
* Corresponding author. E-mail address: treisman@saturn.med.nyu.edu.

© 2004 by The American Society for Cell Biology

threonine protein phosphatase is a heterotrimer consisting of a catalytic subunit (PP1cδ), a 20-kDa protein of unknown function, and the myosin binding subunit (MBS) that targets MLCP to its substrates, which include both MRLC and Moesin (Alessi *et al.*, 1992; Fukata *et al.*, 1998; Hartshorne *et al.*, 1998). Phosphorylation by Rok of a specific threonine within a conserved motif in MBS has been shown to inhibit MLCP activity; this suggests that Rok can positively activate MRLC and Moesin both by direct phosphorylation of these two substrates and also by inhibition of MBS (Feng *et al.*, 1999; Hartshorne *et al.*, 1998; Kawano *et al.*, 1999). Like *zip* mutants, *Drosophila Myosin binding subunit* (*Mbs*) mutants fail to complete dorsal closure, suggesting that this process requires spatially regulated myosin activation (Young *et al.*, 1993; Mizuno *et al.*, 2002; Tan *et al.*, 2003). *Mbs* is also required for the growth of ring canals during oogenesis, and genetic interactions suggest that it opposes the functions in imaginal disc development of *zip*, *Rho1*, and *rok* (Mizuno *et al.*, 2002; Tan *et al.*, 2003). Likewise, *Caenorhabditis elegans mel-11*, which encodes MBS, and *let-502*, which encodes Rok, have opposite functions in embryonic elongation (Wissmann *et al.*, 1999).

Photoreceptor differentiation progresses across the *Drosophila* eye disc from posterior to anterior and is preceded by an epithelial indentation known as the morphogenetic furrow (MF). Cells in the MF undergo a transient contraction along the apical-basal axis and constrict their apical surfaces (Ready *et al.*, 1976). After emerging from the MF, some of these cells assemble into ommatidial clusters, differentiate into photoreceptors, and extend axons through the optic stalk into the brain (reviewed by Wolff *et al.*, 1997). We identified *Mbs* mutations in a screen for genes required for normal photoreceptor differentiation (Janody *et al.*, 2004), and we report here our findings on the role of *Mbs* in photoreceptor development. The results suggest that photoreceptor neurons require *Mbs* to reduce myosin activity and thus prevent their cell bodies from migrating toward their axon terminals.

MATERIALS AND METHODS

Fly Stocks

Fly stocks used include *sqhA21* (Jordan and Karess, 1997), *sqhE20E21* (Winter et al., 2001), *zip*^{1}, *dsh*^{1}, *disco*^{1}, UAS-CD8GFP, *daughterless*-GAL4, *eyeless*-GAL4, *GMR*-GAL4 (Flybase), UAS-*mycMoe*^{T559D}, UAS-*mycMoe*^{T559A} (Speck *et al.*, 2003), *rok*^{2}, and UAS-*rokCAT* (Winter *et al.*, 2001).

Genetics

A complementation group consisting of four alleles was isolated from a mosaic screen for mutations affecting early eye development (Janody *et al.*, 2004) and was found to be allelic to *l(3)72Dd*. These mutations also failed to complement 3 P-element insertions, *l(3)S095304*, *l(3)S041315*, and *l(3)03802*, which were listed in Flybase as or shown by inverse polymerase chain reaction (PCR) to be insertions in the *Mbs* gene, but complemented excisions of these P elements. *Mbs*^{T111} seemed to be weaker than the three alleles used in this article, *Mbs*^{T541}, *Mbs*^{T666}, and *Mbs*^{T791}. *Mbs* mutant eye disc clones were generated by crossing *FRT80*, *Mbs*/TM6B males to *FRT80*, *arm-lacZ*; *ey*FLP1 or *FRT80*, *Ubi-GFP*; *ey*FLP1 females. Positively labeled clones were made by crossing *FRT80*, *Mbs*^{T666}/TM6B; UAS-*CD8GFP* males to *ey*FLP1; *Tub*-GAL4; *FRT80*, *Tub*-GAL80 females. Overexpression of UAS transgenes such as UAS-*rokCAT* specifically in *Mbs* mutant clones was done by crossing *FRT80*, *Mbs*; UAS-*rokCAT*/SM6-TM6B males to *ey*FLP1, UAS-*GFP*; *Tub-GAL4*; *FRT80*, *Tub-GAL80* females. *rok*^{2} eye disc clones resulted from crosses between *FRT19*, *armlacZ/Y*; *ey*FLP/TM6B and *FRT19*, *rok*^{2}/FM7GFP. *Mbs* mutant wing disc clones were generated by crossing *FRT80*, *Mbs*/TM6B males to *FRT80*, *Ubi-GFP; teashirt-GAL4*, UAS-*FLP*/SM6-TM6B females, or to *FRT80*, *P(w+)*, *P(y+)*/TM3; *hs*FLP122 females and heat-shocking the larvae for 1 h at 37°C in both first and second instars. *Mbs* mutant clones in a *disco* background were made by crossing *disco*^{1}; *FRT80*, *Ubi-GFP*/TM6B females to *w*; *ey*FLP2; *FRT80*, *Mbs*^{T666}/TM6B males. Male larvae were dissected.

Immunostaining, Histology, and In Situ Hybridization

Primary antibodies used were rat anti-Elav (1:5; Developmental Studies Hybridoma Bank, Iowa City, IA), mouse anti-Elav (9F8A9; 1:10; Developmental Studies Hybridoma Bank), mouse anti-Neuroglian (BP104; 1:1; Developmental Studies Hybridoma Bank), rabbit anti-β-galactosidase (1:5000; Cappel Laboratories, Durham, NC), mouse anti-β-galactosidase (1:200; Promega, Madison, WI), rabbit anti-Atonal (1:5000; Jarman *et al.*, 1994), rabbit anti-phospho-MRLC (1:10; Cell Signaling Technology, Beverly, MA), rabbit anti-MRLC (1:10, kindly provided by Tien Hsu, Medical University of South Carolina, Charleston, SC), rabbit anti-phospho-ERM (1:5; Cell Signaling Technology), rat anti-Crumbs (F1; 1:100; Pellikka *et al.*, 2002), rat anti-DE-Cadherin (1:20; Oda *et al.*, 1994), rabbit anti-Patj (1:500; Bhat *et al.*, 1999; Pielage *et al.*, 2003), mouse anti-phosphotyrosine (1:100; Upstate Biotechnology, Lake Placid, NY), mouse anti-Nubbin (1:10; Ng *et al.*, 1995), rabbit anti-MHC (1:250; Jordan and Karess, 1997), mouse anti-myc (1:50; Santa Cruz Biotechnology, Santa Cruz, CA), mouse anti-Chaoptin (24B10; 1:50; Developmental Studies Hybridoma Bank), rabbit anti-GFP (1:100; Molecular Probes, Eugene, OR), and mouse anti-GFP (1:100; Santa Cruz Biotechnology). Rhodamine-conjugated phalloidin (Sigma-Aldrich, St. Louis, MO) was used at 0.3 μM. Eye and wing imaginal discs or eye disc-brain complexes were dissected in 0.1 M sodium phosphate buffer (pH 7.2) and then usually fixed in PEM (0.1 M PIPES, pH 7.0, 2 mM $MgSO_4$, 1 mM EGTA) containing 4% formaldehyde with the following exceptions: for phospho-MRLC, MHC, phospho-ERM, DE-Cadherin, and Chaoptin, PLP fixative (75 mM lysine, 37 mM sodium phosphate, pH 7.2, 10 mM sodium *m*-periodate, 2% formaldehyde) was used. For Crumbs staining, discs were fixed in PEM containing 10% formaldehyde. Appropriate horseradish peroxidase- and fluorescent-conjugated secondary antibodies were used (1:200; Jackson ImmunoResearch Laboratories, West Grove, PA). Fluorescent images were collected on a Leica TCS NT confocal microscope and processed using Volocity 2.0.1 or Adobe Photoshop software. Adult wings were mounted in methyl salicylate: Canada balsam (1:2). Digoxigenin-UTP labeled RNA probes homologous to the *Mbs* coding region were used for in situ hybridization to eye discs (Maurel-Zaffran and Treisman, 2000).

Molecular Biology

To identify the molecular alterations of *Mbs* mutant alleles, each was balanced over TM6BGFP. Genomic DNA was prepared from the original isogenic *FRT80* flies and from homozygous mutant embryos, and the *Mbs* exons were amplified by PCR and sequenced. The *Mbs* sequence was obtained from two Berkeley *Drosophila* Genome Project cDNA clones (RE63915 and AT12677). The cDNA from AT12677 lacks a 129-amino acid exon in the central region (Figure 2A). The full-length *Mbs* cDNA was amplified by PCR from the RE63915 clone with Pfu Turbo (Stratagene, La Jolla, CA) and cloned into HA-pUAST as a *Nde*I/*Kpn*I fragment to generate UAS-*Mbs*. To generate UAS-*MbsN300*, the N-terminal 300 amino acids of Mbs were amplified and cloned into HA-pUAST as a *Nde*I/*Xba*I fragment.

Genetic Interaction Analyses

For *dsh*^{1} interactions, cells with multiple wing hairs were counted on both the ventral and dorsal surfaces of the wing area demarcated by the third and fifth longitudinal wing veins, the cross veins, and the wing margin. In total, 21 wings per genotype were counted. For *sqh* transgenes, the ommatidia missing from the apical level in *Mbs* mutant eye disc clones were divided by the total number of ommatidia expected in the clones. At least 15 eye discs per genotype were counted. In both cases, statistical significance was determined by unpaired Student's *t* test.

RESULTS

Mbs Mutant Photoreceptors Lose Their Apical Localization but Maintain Their Polarity

We have carried out a mosaic genetic screen to identify genes required for the normal pattern of photoreceptor differentiation (Janody *et al.*, 2004). In this screen, we isolated four alleles of *Myosin binding subunit* (*Mbs*), which encodes a subunit of the *Drosophila* myosin light chain phosphatase enzyme. Loss of *Mbs* led to an apparent reduction in photoreceptor differentiation in mutant clones in the eye disc, as evidenced by staining with the neuronal nuclear marker Elav (Figure 1, A–C). However, expression of the bHLH transcription factor Atonal, an early marker of differentiation (Jarman *et al.*, 1994), was largely normal even in eye discs containing very large *Mbs* clones generated in a *Minute* background (our unpublished data). In the apical region of the eye disc, *Mbs* mutant clones showed a reduction in both the number of ommatidial clusters and the number of Elav-

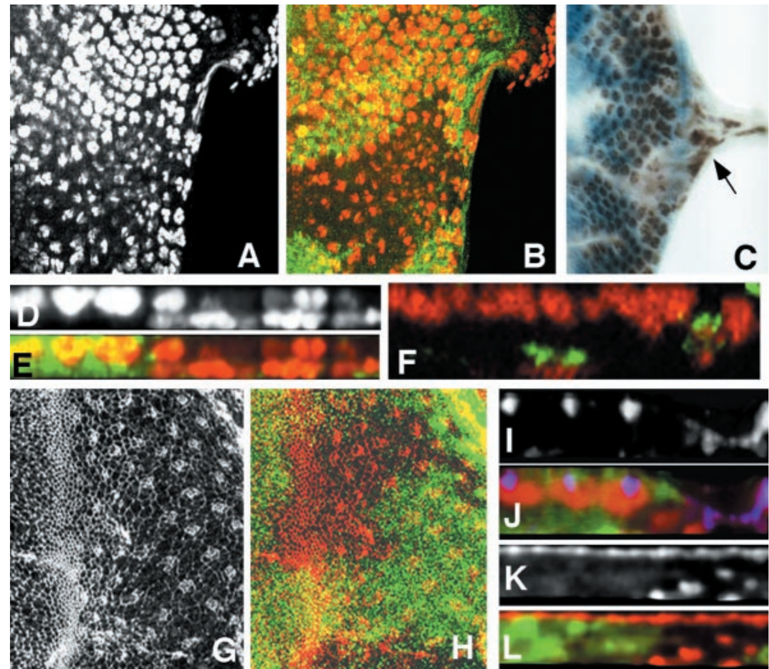

Figure 1. *Mbs* mutant photoreceptors move basally and into the optic stalk. (A–C) Eye discs with Mbs^{T666} clones stained with anti-Elav to label photoreceptor nuclei (A, red in B, brown in C). Wild-type tissue is marked with *arm-lacZ*, stained with anti-β-galactosidase in green (B) or X-gal in blue (C). Posterior is to the right. Many mutant cells are lost from the apical layer, and some Elav-positive nuclei are present in the optic stalk (arrow in C). (D and E) show cross sections of the discs in A and B, with apical up. Wild-type nuclei are close to the apical surface, but many mutant nuclei are found close to the basal surface. (F) Cross-section of an eye disc with Mbs^{T666} mutant cells positively marked with CD8-GFP (green). Elav is stained in red. The entire membrane of *Mbs* mutant cells seems to be located basally within the disc. (G and H) Eye discs with Mbs^{T666} clones stained with anti-phosphotyrosine (G, red in H) and with anti-β-galactosidase, marking wild-type tissue, in green in H. Apical constriction in the furrow is slightly reduced in the mutant tissue, and no ectopic constriction is visible in posterior regions. (I–L) Cross-sections of discs with Mbs^{T541} clones stained with anti-E-cadherin (I, blue in J), anti-Elav (red in J), anti-Patj (K, red in L), and anti-β-galactosidase to mark wild-type tissue (green in J and L). E-cadherin and Patj are still expressed in mutant tissue, but at a more basal level than in wild-type tissue; staining is apical to mislocalized nuclei (J).

expressing nuclei within each cluster. However, we found that clusters of photoreceptor nuclei were present at a more basal level. This could be most easily visualized in cross-sections of the tissue (Figure 1, D and E). Ectopic Elav staining also was detected in the optic stalk, where it is normally absent (Figure 1C).

We considered several possible explanations of these results. First, because myosin can control cell shape through its interactions with actin filaments, we thought that the basal localization of *Mbs* mutant photoreceptor nuclei might be caused by cell shape changes such as those that normally occur in the MF. To look at cell shape, we stained *Mbs* mutant clones with anti-phosphotyrosine (p-Tyr) antibody, which outlines apical cell membranes, and phalloidin, which marks actin filaments. We saw only a slight reduction in apical constriction in the MF in *Mbs* mutant clones, and no ectopic apical constriction in more posterior regions of the disc (Figure 1, G and H; our unpublished data). Thus, cell shape changes are unlikely to be responsible for the altered nuclear localization of *Mbs* mutant photoreceptors.

Another possibility is that *Mbs* mutant photoreceptors might undergo an epithelial to mesenchymal transition, permitting them to migrate basally and through the optic stalk. This would resemble the phenotype of wing disc cells mutant for *Moesin* (*Moe*), which encodes a reported substrate of myosin light chain phosphatase (Fukata *et al*., 1998; Speck *et al*., 2003). However, we found that basally located *Mbs* mutant photoreceptors retained at least some elements of their epithelial character and their polarity, as indicated by Pals-associated tight junction protein (Patj), Crumbs, and DE-Cadherin staining (Muller, 2003). These markers of the apical membrane were still present above mislocalized nuclei, but below the level at which they are found in wild-type tissue (Figure 1, I–L; our unpublished data). These results also suggested that the entire *Mbs* mutant cell was mislocalized, rather than just the nucleus. Positively labeling mutant cells with the membrane marker CD8-GFP supported this conclusion, because some mutant cells had no visible contact with the apical surface of the epithelium (Figure 1F). *Mbs* mutant photoreceptors thus seem to leave the epithelium and move into the optic stalk without becoming mesenchymal.

Loss of Myosin Binding Subunit Causes the Mutant Eye Phenotype

Like the myosin binding subunits of other species, *Drosophila* Mbs contains multiple N-terminal ankyrin repeats, a conserved motif (RRSTQGVTL) surrounding the key inhibitory threonine site, T_{593}, and a C-terminal domain similar to a leucine zipper (Figure 2A; Shimizu *et al*., 1994; Fujioka *et al*., 1998; Hartshorne *et al*., 1998). The first 300 amino acids of Mbs are sufficient for constitutive myosin phosphatase activity (Tanaka *et al*., 1998; Totsukawa *et al*., 2000). To determine the nature of our *Mbs* alleles, we sequenced genomic DNA from homozygous mutant embryos. We found that Mbs^{T541}, Mbs^{T666}, and Mbs^{T791} each introduce a stop codon within the first 250 amino acids of Mbs and thus are likely to be null alleles (Figure 2A). These three alleles had indistinguishable mutant phenotypes in the eye disc. We also showed by in situ hybridization that *Mbs* is expressed at a low level throughout the third instar eye disc (Figure 2, B and C).

We generated transgenic fly lines expressing either the full-length *Mbs* cDNA (including an alternatively spliced exon) (Mizuno *et al*., 2002) or a truncated form of *Mbs* predicted to be constitutively active (MbsN300) under the control of UAS sites (Figure 2A). Ubiquitous expression of full-length *Mbs* driven by *daughterless* (*da*)-GAL4 partially rescued the embryonic lethality of *Mbs* trans-heterozygotes, allowing survival to the pupal or adult stages (Table 1). We also showed that expression of UAS-*Mbs* specifically in *Mbs* mutant eye disc clones using the MARCM system (Lee and Luo, 1999) rescued eye development; cross-sections showed that *Mbs* mutant photoreceptor nuclei were restored to their normal apical level (Figure 2, D–G). These results confirm that the photoreceptor phenotype is due to loss of *Mbs* activity. Ubiquitous expression of *Mbs* in wild-type flies had no phenotype, whereas expression of *MbsN300* caused lethality at or before the pupal stage (Table 1); this would be

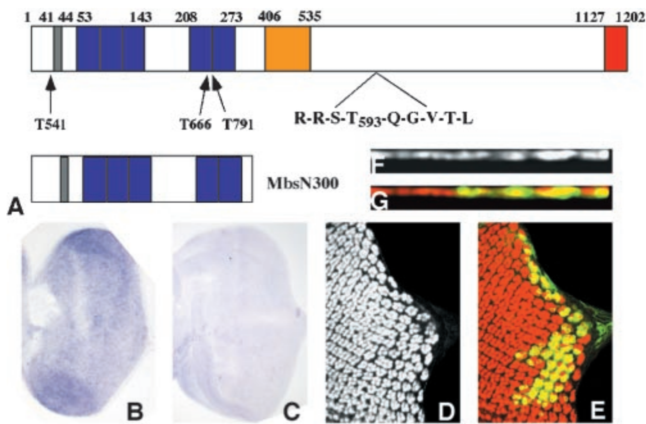

Figure 2. Loss of *Mbs* causes the eye disc phenotype. (A) Diagram of the Mbs protein, with the PP1cδ binding motif shown in gray, ankyrin repeats in purple, an alternatively spliced 129 amino acid exon in yellow, and a conserved leucine zipper motif in red. The sequence around the phosphorylation site, T_{593}, is enlarged, and the positions of stop codons introduced by the Mbs^{T541} (W22), Mbs^{T666} (Q239) and Mbs^{T791} (W243) alleles are indicated. The structure of the truncated protein MbsN300 is shown below. (B and C) In situ hybridization to third instar eye discs with antisense (B) and sense (C) *Mbs* probes. A low level of *Mbs* RNA is present throughout the disc. (D–G) Clones mutant for Mbs^{T666} and expressing UAS-*Mbs* with *tub*-GAL4, positively labeled with UAS-GFP in green (E and G) and stained for Elav (D and F, red in E and G). Top views are shown in D and E and cross sections in F and G. Nuclei are restored to their apical position by expression of *Mbs* (compare to Figure 1, A–E).

consistent with MbsN300 exhibiting unregulated activity. However, expression of *MbsN300* in the eye disc with *eyeless*-GAL4 or *GMR*-GAL4 caused no apparent defects in photoreceptor differentiation (our unpublished data).

Mbs Is Not Required for the Apical Localization of Wing Disc Cells

To determine whether *Mbs* affected the apical localization of cells in other epithelial tissues, we examined its effect on the wing imaginal disc. *Mbs* mutant clones in adult wings produced stunted and forked wing hairs (Figure 3A). To ascertain whether this phenotype was due to loss of apical localization of wing disc cells, we stained *Mbs* mutant clones in the wing disc with an antibody to the nuclear transcription factor Nubbin (Ng *et al.*, 1995). Cross-sections of these clones demonstrated that the wing cell nuclei were all still present at the same position as in wild-type tissue (Figure 3, B and C). This result was further supported by the normal apical localization of Crumbs and DE-Cadherin in *Mbs* mutant cells (Figure 3, D and E; our unpublished data). These data indicate that the *Mbs* mutant eye phenotype must result from a mechanism absent in the wing.

Drosophila myosin II, encoded by *zipper* (*zip*), has been shown to act downstream of *dishevelled* (*dsh*) in the control of wing hair number; reducing *zip* dosage enhances the multiple hair phenotype induced by loss of *dsh* (Winter *et al.*, 2001). We therefore tested whether enhancing myosin activity by reducing *Mbs* dosage might have the opposite effect on *dsh*. We found that removing one copy of *Mbs* attenuated the multiple wing hair phenotype of dsh^1 mutants by 50–60% (Figure 3, H–J). This indicates that *Mbs* functions downstream of *dsh* to antagonize its block of multiple hair formation. However, like other myosin regulators (Winter *et al.*, 2001), *Mbs* had no effect on the planar polarity defects of dsh^1.

Mbs Mediates Its Effects on the Eye through Sqh Dephosphorylation

Two substrates for the phosphatase activity of MLCP have been described based on in vitro biochemical experiments: MRLC, encoded in *Drosophila* by *spaghetti squash* (*sqh*; Karess *et al.*, 1991), and the ERM protein Moe (Fukata *et al.*, 1998; Hartshorne *et al.*, 1998). To test whether one of these proteins was the primary target of Mbs in the eye disc, we first used phospho-specific antibodies to examine their phosphorylation state in *Mbs* mutant cells. High levels of phosphorylated Sqh (p-Sqh) are normally restricted to cells in the MF; however, p-Sqh staining was greatly increased in *Mbs* mutant clones both anterior and posterior to the MF (Figure 4, A–D). The level of Sqh itself, visualized with a nonphospho-specific antibody, was not altered (our unpublished data). Abnormally high levels of p-Sqh staining were also visible in *Mbs* mutant clones in the wing disc (Figure 3, F and G). In contrast, we detected no increase in phosphorylated Moe (p-Moe) levels in *Mbs* mutant clones (Figure 4, E and H). p-Moe staining was observed both in the undifferentiated cells that surround each ommatidium (Figure 4, E and F), and in the apical regions of photoreceptor clusters (Figure 4, G and H). These results show that *Mbs* is necessary to restrict the phosphorylation of Sqh, but not Moe, in the eye disc.

We obtained further evidence that Mbs acts through Sqh by looking at the effects of *sqh* transgenes with phosphorylation site mutations on the *Mbs* mutant phenotype. Previous biochemical and genetic studies have shown that serine 21 and threonine 20 are the conserved primary and secondary phosphorylation sites, respectively (Pearson *et al.*, 1984;

Table 1. Mbs rescues the lethality of *Mbs* mutants and antagonizes Rok function

Rescue of Lethality	Pupal stage	Adulthood
da-GAL4, Mbs^{T791}/TM6B X *Mbs^{T541}/TM6B*	0/191 (0%)[a]	0/120 (0%)[a]
da-GAL4, Mbs^{T791}/TM6B X *UAS-Mbs1, Mbs^{T541}/TM6B*	96/305 (91%)	32/175 (45%)
da-GAL4 X *UAS-Mbs1/TM6B*	123/225 (121%)	111/190 (141%)
da-GAL4, Mbs^{T541}/TM6B X *Mbs^{T666}/TM6B*	0/404 (0%)	0/237 (0%)
da-GAL4, Mbs^{T541}/TM6B X *UAS-Mbs2, Mbs^{T666}/TM6B*	43/151 (80%)	3/99 (6%)
da-GAL4 X *UAS-MbsN300/TM6B*	195/467 (72%)	0/219 (0%)
da-GAL4 X *UAS-rokCAT/TM6B*	33/308 (12%)	0/167 (0%)
da-GAL4 X *UAS-MbsN300, UAS-rokCAT/TM6B*	372/928 (67%)	118/499 (31%)

[a] The number of nonbalancer flies reaching pupation or adulthood is shown over the total number of flies at that stage. Survival is shown as a percentage of the expected number of nonbalancer flies in parentheses.

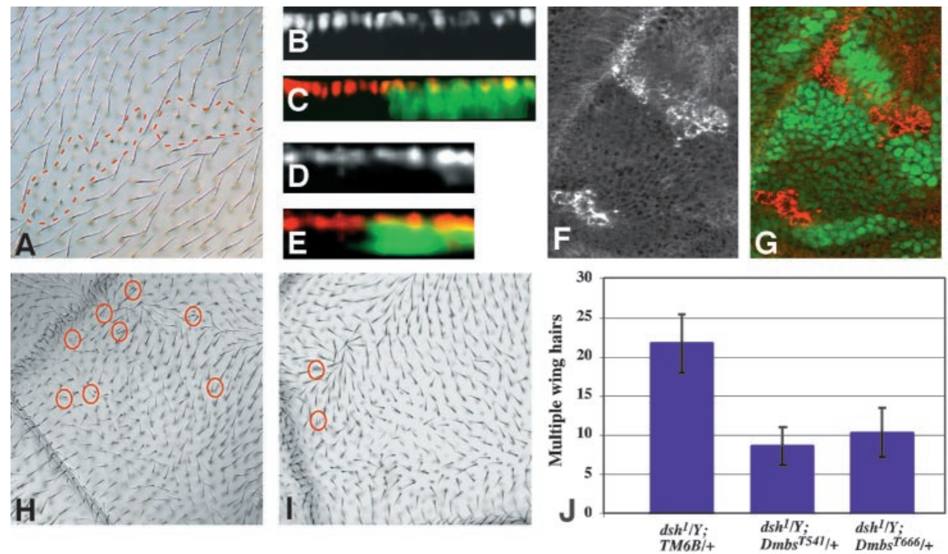

Figure 3. *Mbs* affects wing hair development but not the wing disc epithelium. (A) Mbs^{T666} mutant clones in an adult wing. The clones are unmarked, but can be identified by the short and sometimes forked wing hairs (outlined with red dashed lines). (B–E) Cross sections of third instar wing discs containing Mbs^{T666} mutant clones, with wild-type tissue labeled with GFP in green in C and E. Nuclei are stained with anti-Nubbin (B, red in C), and the apical surface is stained with anti-E-cadherin (D, red in E). No alterations in apical/basal localization are apparent within the clones. (F and G) Phospho-MRLC antibody staining of Mbs^{T666} clones in the wing disc (F, red in G). Wild-type tissue is marked with GFP (green in G). p-Sqh is strongly up-regulated in the clones. (H) Multiple wing hair formation and altered polarity in a dsh^1/Y mutant wing. (I) Suppression of multiple hairs, but not polarity, in dsh^1/Y; Mbs^{T541}/+. Examples of duplicated wing hairs are circled in red. (J) Quantification of the suppression of dsh^1 multiple wing hairs in *Mbs* heterozygotes. Wing hairs were counted in a region bordered by veins 3 and 5, the cross-veins and the wing margin.

Ikebe *et al*., 1986; Amano *et al*., 1996; Jordan and Karess, 1997). We therefore made use of *sqhA21*, an inactivating mutation in which serine 21 is changed to alanine, and *sqhE20E21*, a phosphomimetic mutation in which both amino acids are changed to glutamic acid (Jordan and Karess, 1997; Winter *et al*., 2001). These two transgenes are expressed from the endogenous *sqh* promoter. Neither had any visible effect on eye development when one copy was present in an otherwise wild-type background (our unpublished data). We reasoned that if Sqh is the main downstream effector for Mbs in the eye, then the consequences of loss of Mbs function might be ameliorated by the presence of an inactive form of Sqh. Indeed, many *Mbs* mutant photoreceptor nuclei were restored to their normal apical location when they contained a *sqhA21* transgene (Figure 4, I–L). Quantitative analysis showed that the presence of *sqhA21* in *Mbs* mutant clones reduced the number of ommatidia missing from the apical level by ~32% (Figure 4U). However, high levels of p-Sqh staining were still observed in these cells (our unpublished data). This suggests that SqhA21 exerts its effect by binding to downstream effector molecules such as the myosin heavy chain Zip, rather than by blocking the phosphorylation of wild-type Sqh. Introduction of *sqhE20E21* had the opposite effect, enhancing the mislocalization of *Mbs* mutant photoreceptors. Many more photoreceptor nuclei were missing from the apical level, and staining was instead observed in basal regions of the eye disc (Figure 4, M–P, and U).

These data support the model that excessive Sqh phosphorylation is the major cause of the *Mbs* mutant phenotype. In contrast, when we expressed the corresponding inactive and phosphomimetic forms of Moe (UAS-*mycMoeT559A* and UAS-*mycMoeT559D*, respectively) by using the MARCM system (Lee and Luo, 1999; Speck *et al*., 2003), we observed no obvious attenuation or enhancement of the eye phenotype (Figure 4, Q–T). Expression of the transgenes was confirmed by staining with an antibody to the Myc epitope tag (our unpublished data). We thus have no evidence that Moe dephosphorylation by Mbs has any role in maintaining the apical localization of photoreceptor cell bodies.

Mbs Acts through Zip and Is Antagonized by Rok and Other Kinases

The major role of MRLC phosphorylation is thought to be the activation of MHC (Craig *et al*., 1983; Jordan and Karess, 1997). We therefore examined the role of the MHC Zip in generating the abnormal localization of *Mbs* mutant photoreceptors by making *Mbs* mutant clones that were heterozygous for zip^1. As expected, loss of one copy of *zip* significantly improved the eye phenotype; cross sections revealed that *Mbs* mutant photoreceptor nuclei were restored to the apical level (Figure 5, A–D). Only 14% of 71 mutant ommatidia were missing from the apical level. This provides additional evidence that Mbs functions through myosin II to maintain the apical localization of photoreceptors. Because we saw no effect on the level or distribution of Zip protein in *Mbs* clones (our unpublished data), Mbs is likely to act by regulating the activity of Zip through its effect on Sqh.

The critical kinase for Sqh in wing hair development seems to be Rok (Winter *et al*., 2001); Rok might therefore antagonize the activity of Mbs. To test this, we used transgenes expressing activated forms of each protein, the catalytic domain of Rok (RokCAT) or a truncated form of Mbs predicted to be constitutively active (MbsN300; Figure 2A). Ubiquitous expression of either gene led to pupal lethality, although Elav staining of the third instar eye disc seemed normal. However, overexpression of both transgenes allowed ~30% survival to adulthood, suggesting that Rok and Mbs counteract each other's activity, perhaps by acting on common substrates (Table 1). Although Rok can also directly phosphorylate and inactivate Mbs (Feng *et al*., 1999; Kawano *et al*., 1999), its target site is not present in the truncated Mbs protein.

Loss of *rok* produces an eye phenotype much milder than loss of *zip*, affecting ommatidial spacing and photoreceptor number but not cytokinesis (Winter *et al*., 2001). We therefore wondered whether Rok was the major kinase responsible for the phosphorylation of Sqh in the eye disc. Surprisingly, p-Sqh staining was not altered in clones mutant for a null allele of *rok*, rok^2 (Figure 5, E–F). This suggests that another kinase can phosphorylate Sqh in the eye disc. Consistent with this, we did not see a significant enhancement of

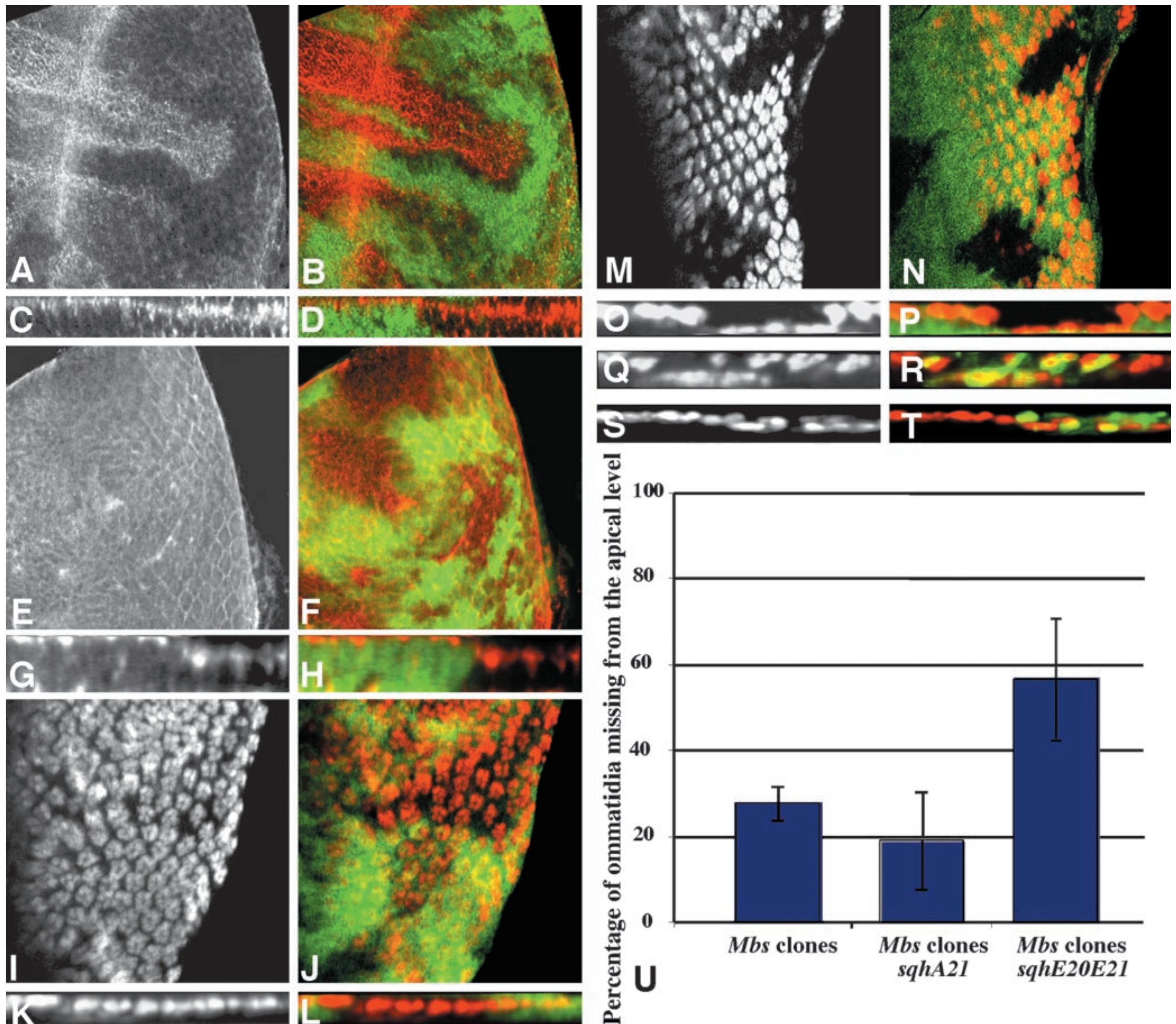

Figure 4. Sqh is the critical substrate for Mbs in eye development. (A–P) Eye discs containing *Mbs* clones, with wild-type tissue marked with anti-β-galactosidase staining in green (B, D, F, H, J, L, N, and P). (A–D) Mbs^{T666} clones stained with an antibody to phospho-MRLC (A and C, red in B and D). (E–H) Mbs^{T541} clones stained with an antibody to phospho-ERM (E and G red in F and H). Cross sections of the discs in A and B are shown in C and D, and cross sections of the discs in E and F are shown in G and H. p-Sqh is strongly up-regulated in *Mbs* clones, but the levels of p-Moe are unaffected, although p-Moe staining is normally at the apical surface and seems more basal in the clones. (I–L) show eye discs carrying the *sqhA21* transgene and containing Mbs^{T541} clones. Anti-Elav staining marks photoreceptor nuclei (I and K and red in J and L). (K and L) Cross sections of the disc in I and J. (M–P) Eye discs carrying the *sqhE20E21* transgene and containing Mbs^{T666} clones. Anti-Elav staining marks photoreceptor nuclei (M and O and red in N and P). (O and P) Cross sections of the disc in M and N. Nuclei are largely restored to the apical layer in *Mbs* clones by the presence of *sqhA21* but are predominantly basal in the presence of *sqhE20E21*. (Q–T) Cross sections of eye discs containing Mbs^{T666} clones, positively marked with GFP (green in R and T) and also expressing UAS-*mycmoeT559A* (Q and R) or UAS-*mycmoeT559D* (S and T) driven by *tub*-GAL4. Anti-Elav staining marks photoreceptor nuclei (Q and S and red in R and T). Neither transgene obviously alters the severity of the *Mbs* phenotype. (T) Quantification of the proportion of ommatidia completely missing from the apical layer in *Mbs* clones in a wild-type background or in a *sqhA21* or *sqhE20E21* background. $p < 0.01$ for a comparison of *sqhA21* to wild type, and $p < 0.001$ for a comparison of *sqhE20E21* to wild type.

the photoreceptor localization defect in *Mbs* mutant clones expressing RokCAT (Figure 5, G–H).

Mbs *Mutant Cell Bodies Move toward Their Axon Terminals*

Because the apical localization of photoreceptors, but not wing disc cells, requires *Mbs*, we considered the possibility that axon extension was important in directing the movement of *Mbs* mutant cell bodies. *Mbs* mutant cell bodies indeed seemed to move toward their axon terminals, because they were found in the optic stalk and even within the lamina (Figure 6A). However, loss of *Mbs* does not seem to cause overextension of axons, as the terminals of these mislocalized cells were present within the region of the wild-type projection (Figure 6A).

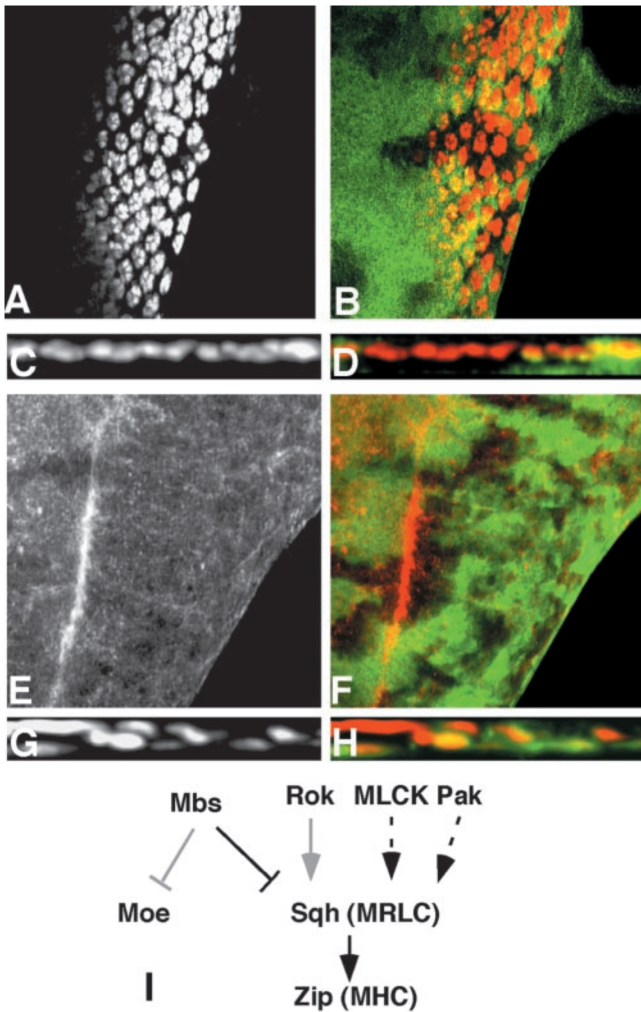

Figure 5. Zip acts downstream of Mbs, but Rok is not the only upstream regulator of Sqh. (A–D) show eye discs heterozygous for *zip*^{1} and containing *Mbs*^{T541} clones, with wild-type tissue marked with anti-β-galactosidase staining in green (B and D). Anti-Elav staining marks photoreceptor nuclei (A and C and red in B and D). (C and D) Cross sections of the disc in A and B. Removal of one copy of *zip* strongly suppresses the photoreceptor localization defect of *Mbs* mutant clones. (E and F) show an eye disc containing *rok*^{2} clones, with wild-type tissue marked with GFP (green in F). Phospho-MRLC is stained (E, red in F). p-Sqh is not obviously reduced in the absence of *rok*. (G and H) Cross sections of eye discs containing *Mbs*^{T541} clones, positively marked with GFP (green in H) and also expressing UAS-*RokCAT* driven by *tub*-GAL4. Anti-Elav staining marks photoreceptor nuclei (G and red in H). Activated Rok does not strongly enhance the phenotype of loss of *Mbs*. (I) Functional relationships between components of the Mbs pathway. Arrows indicate activation and perpendicular lines inhibition. Black is used for interactions demonstrated to be important in the eye disc, gray for interactions that do not seem to occur in the eye disc, and dashed lines indicate possible interactions.

The best test of whether axon outgrowth is required for the *Mbs* phenotype would be to determine whether *Mbs* mutant photoreceptors remain within the epithelium when axon outgrowth is prevented. However, there is currently no way to completely block axon outgrowth, and most methods that produce a partial block also would cause other disruptions of the cytoskeleton (Kim *et al*., 2001; Lee and Kolodziej, 2002). As an alternative, we generated *Mbs* clones in a *disconnected* (*disco*) mutant background. In *disco* mutants, the optic stalk is absent and the photoreceptor axons remain within the eye disc, where they extend and form basal tangles (Steller *et al*., 1987). However, the focus of *disco* activity is in the optic lobe pioneer neurons in the brain, and the photoreceptors themselves are normal (Campos *et al*., 1995). In this background, *Mbs* mutant photoreceptors still moved basally within the eye disc (Figure 6, B–F). However, rather than moving toward the site of the optic stalk, the mutant nuclei were found more centrally at the basal surface of the eye disc, and were concentrated at sites where many axons were present (Figure 6F). This rules out the possibility that the posterior eye disc produces an attractant for the mutant photoreceptors, and suggests that the location of the axon terminals directs the movement of the cell bodies.

DISCUSSION

Mbs Functions to Limit Myosin Activity in the Eye Disc

We have shown that Mbs exerts its effects on eye development by regulating the phosphorylation state of the Sqh MRLC subunit of nonmuscle myosin II. The level of phosphorylated Sqh is greatly increased in *Mbs* mutant clones in both the eye and wing discs, and nonphosphorylatable or phosphomimetic forms of Sqh strongly modulate the severity of the *Mbs* phenotype (Figure 4). In addition, the effect of *zip* dosage on the *Mbs* phenotype indicates that p-Sqh acts through Zip to control photoreceptor localization. It also has been shown that rat Mbs can bind to and dephosphorylate Moesin in vitro, and it was suggested that Mbs might mediate regulation of Moesin by Rho (Fukata *et al*., 1998). However, our in vivo data show that in the eye disc Mbs is not required to dephosphorylate Moe. If dephosphorylation of Moe by Mbs occurs in vivo, it may be limited to specific tissues or developmental stages.

The identity of the kinase antagonized by Mbs in the eye is less clear (Figure 5I). Although it has been reported that Rok can phosphorylate Sqh in vitro and that p-Sqh levels are reduced in *rok* mutant larvae (Mizuno *et al*., 1999; Winter *et al*., 2001), we detected normal levels of p-Sqh in *rok*^{2} eye disc clones. In addition, overexpression of Rok-CAT in the eye disc had no visible effect on photoreceptor differentiation or localization (our unpublished data), and did not seem to enhance the *Mbs* phenotype. Consistent with these results, another group observed little effect of *Mbs* dosage on the photoreceptor phenotype caused by Rho activation in the eye disc (Tan *et al*., 2003). Rok may have a more significant effect on Sqh phosphorylation in other tissues; we found that the lethality caused by overexpression of constitutively active Mbs was partially suppressed by coexpression of the catalytic domain of Rok. Myosin seems to be a downstream effector of Rho and Rok in wing and leg development (Halsell *et al*., 2000; Winter *et al*., 2001), and the MEL-11 myosin phosphatase antagonizes the LET-502 Rho kinase in *C. elegans* development (Piekny *et al*., 2000), supporting a role for Rok in phosphorylating Sqh in some cell types.

Another kinase that might phosphorylate Sqh in the eye disc is MLCK. It has been reported that MLCK phosphorylates MRLC at the periphery of fibroblast cells, whereas ROCK acts in the central domain of these cells (Totsukawa *et al*., 2000). *Drosophila Stretchin-MLCK* is a very large compound gene that produces multiple alternatively spliced transcripts (Champagne *et al*., 2000), and no mutations in this gene have been identified, preventing us from analyzing its interactions with *Mbs*. Another possible kinase is p21-activated kinase (PAK), which has been shown to increase

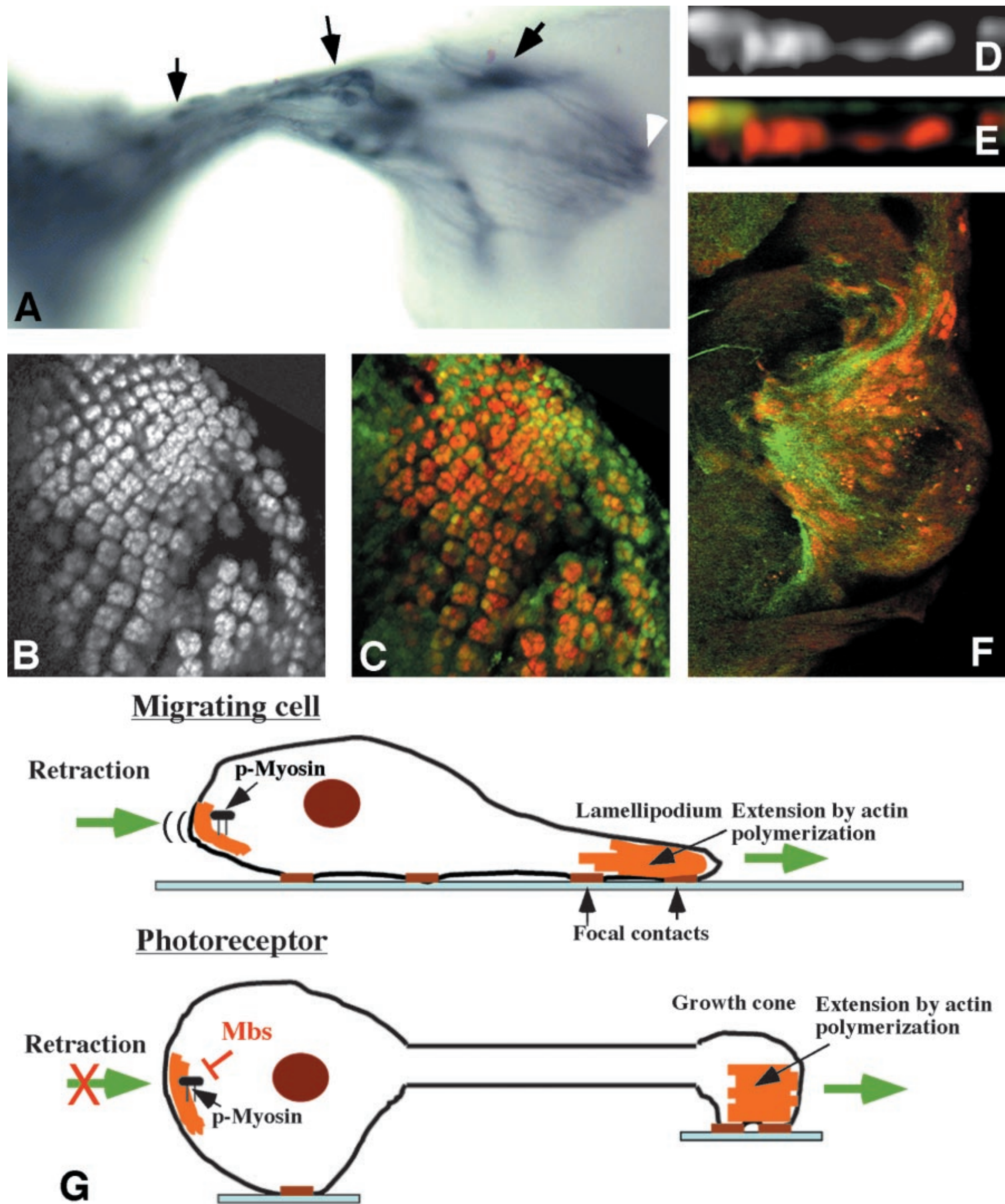

Figure 6. *Mbs* mutant photoreceptors move toward their axon terminals. (A) Third instar eye disc-brain complex containing unmarked Mbs^{T541} clones, stained with anti-Chaoptin to label all photoreceptor cell membranes. Mislocalized cell bodies are visible within the optic stalk and the lamina (arrows). The latter cells project into the medulla (white arrowhead). (B–F) Eye discs containing Mbs^{T666} clones generated in a $disco^{1}$ background. Photoreceptors are stained with anti-Elav (B and D, red in C, E, and F), and wild-type tissue is marked with GFP in green (C and E). Photoreceptors still move basally in *disco* mutants. (F) Basal focal plane with axons stained with anti-Chaoptin (green). Mislocalized nuclei are present close to a concentration of axons. (G) Comparison of cell migration to neuronal axon extension. Actin polymerization is important to extend the leading edge of a migrating cell and the growth cone of a neuron. During cell migration, phosphorylated myosin retracts the rear of the cell. Mbs may prevent a similar retraction of neuronal cell bodies.

the level of phosphorylated MRLC in cultured cells (Kiosses *et al*., 1999) and to phosphorylate MRLC in vitro (Chew *et al*., 1998; Crawford *et al*., 2001). Interestingly, overexpression of a myristylated form of PAK in *Drosophila* photoreceptors causes their cell bodies to detach from the eye disc epithelium and enter the brain, strongly resembling the *Mbs* mutant phenotype (Hing *et al*., 1999). *Pak* mutant photoreceptors develop normally except for axon guidance defects (Hing *et al*., 1999), suggesting that *Pak* is not essential for myosin activation in these cells. However, a second *Pak*

gene, *mushroom bodies tiny*, is required for late photoreceptor morphogenesis and adherens junction integrity (Schneeberger and Raabe, 2003), and a third *Pak* gene is present in the genome, raising the possibility that these enzymes have redundant functions and complicating any analysis of their interactions with *Mbs*.

Mbs Prevents Loss of Photoreceptors from the Eye Disc Epithelium

The excessive myosin activity present in *Mbs* mutant photoreceptors causes them to adopt a more basal location in the eye disc and sometimes to enter the optic stalk. We have addressed several possible mechanisms for this phenotype. Myosin can affect the shape of cultured cells by promoting the assembly of stress fibers and focal adhesions (Eto *et al*., 2000; Totsukawa *et al*., 2000), and a transient accumulation of p-Sqh accompanies the apical constriction and apical-basal contraction of cells in the morphogenetic furrow (Figures 4A and 5F). We therefore wondered whether loss of *Mbs* might induce these cell shape changes in ectopic regions of the eye disc, resulting in mutant cells that formed a constitutive furrow. However, visualization of the apical surface of mutant clones by p-Tyr or phalloidin staining did not reveal any ectopic apical constriction of cells surrounding the photoreceptor clusters, suggesting that myosin phosphorylation is not sufficient to induce the cell shape changes that occur in the morphogenetic furrow. In addition, the integrity of the epithelial surface surrounding the photoreceptor clusters indicates that loss of *Mbs* specifically affects the localization of photoreceptor cells.

Another possibility was that *Mbs* mutant cells might undergo an epithelial to mesenchymal transition and become migratory. This phenotype has been reported for wing disc cells mutant for *Moe*, which encodes a potential substrate of Mbs (Fukata *et al*., 1998; Speck *et al*., 2003). However, *Mbs* mutant cells in the wing disc remain within the epithelium and show no change in their apical-basal localization, although p-Sqh is up-regulated to a similar extent in both the wing and eye discs. In addition, *Mbs* mutant photoreceptors seem to retain some aspects of their epithelial character; they continue to express the epithelial apical junction proteins Patj, Crumbs, and E-cadherin (Muller, 2003; Figure 1, and our unpublished data). These proteins are present apical to mislocalized nuclei, suggesting that the entire cell is affected rather than the position of the nucleus within the cell. In contrast, the nuclei of *klarsicht* or *Glued* mutant cells are basally located within the cell due to defective dynein function (Fan and Ready, 1997; Mosley-Bishop *et al*., 1999).

The model we favor is that unregulated myosin generates a traction force that pulls photoreceptor cell bodies toward their axon terminals. This would explain why the *Mbs* phenotype is specific to photoreceptors rather than wing disc cells or undifferentiated cells in the eye disc. It also would explain why the movement of mutant cells is directed toward the optic stalk or, in a *disco* background, toward the axon terminals within the eye disc. This abnormal force also might be accompanied by changes in adhesion to other cells or the substrate. Loss of *Mbs* could reduce the adhesion of epithelial cells to their neighbors, preventing them from withstanding the normal forces involved in axon extension. However, *Mbs* clones do not show the smooth borders characteristic of changes in adhesive properties (Dahmann and Basler, 1999).

We do not know whether the force generated by excessive myosin activity is located at the growth cone or in the cell body, although we favor the latter model because the highest levels of p-Sqh are found in apical regions of both wild-type and *Mbs* mutant cells (Figure 4, C and D). In vertebrate growth cones, two isoforms of the heavy chain of nonmuscle myosin II seem to have different locations and functions (Brown and Bridgman, 2003a). MHCIIB is more peripheral and is required for axon outgrowth, whereas MHCIIA is central and is required for cell adhesion (Rochlin *et al*., 1995; Wylie *et al*., 1998; Bridgman *et al*., 2001; Wylie and Chantler, 2001; Brown and Bridgman, 2003b). *Drosophila* has only a single *zip* gene, which may perform both functions. The importance of MHCIIB in generating the traction force that allows growth cone extension (Bridgman *et al*., 2001) suggests that this force might be increased in the absence of MLCP activity. There is a precedent for the idea that axon outgrowth can exert a pulling force on the cell body, because it has been shown that chick motor neurons will migrate out of the spinal cord along their axons if their movement is not blocked by boundary cap cells (Vermeren *et al*., 2003).

The other possibility is that the actomyosin contraction takes place within the cell body, detaching it from surrounding cells and pulling it toward the growth cone. This would resemble the normal function of myosin in retracting the rear of migrating cells (Kolega, 2003; Ridley *et al*., 2003; Uchida *et al*., 2003). Cell detachment and shrinkage has been reported for fibroblasts treated with an inhibitor of MLCP activity (Eto *et al*., 2000). Myosin light chain phosphatase activity may be specifically required in neuronal cells to allow axon extension to occur without triggering a migratory response in the cell body (Figure 6G).

ACKNOWLEDGMENTS

We thank Steve Cohen, Richard Fehon, Tien Hsu, Brad Jones, Roger Karess, Dan Kiehart, Liqun Luo, Thomas Marty, Javier Morante, François Payre, Ulrich Tepass, Mark VanBerkum, the Bloomington *Drosophila* stock center, and the Developmental Studies Hybridoma Bank for fly stocks and reagents. We are grateful to Ruth Lehmann for the use of her confocal microscope. We thank Zara Martirosyan and Neal Jahren for technical assistance. The manuscript was improved by the critical comments of Inés Carrera, Kerstin Hofmeyer, Florence Janody, Grant Miura, and Jean-Yves Roignant. This work was supported by National Institutes of Health grants EY-13777 and GM-56131.

REFERENCES

Adelstein, R.S., and Conti, M.A. (1975). Phosphorylation of platelet myosin increases actin-activated myosin ATPase activity. Nature *25*, 597–598.

Alessi, D., MacDougall, L.K., Sola, M.M., Ikebe, M., and Cohen, P. (1992). The control of protein phosphatase-1 by targetting subunits. The major myosin phosphatase in avian smooth muscle is a novel form of protein phosphatase-1. Eur. J. Biochem. *210*, 1023–1035.

Amano, M., Ito, M., Kimura, K., Fukata, Y., Chihara, K., Nakano, T., Matsuura, Y., and Kaibuchi, K. (1996). Phosphorylation and activation of myosin by Rho-associated kinase (Rho-kinase). J. Biol. Chem. *271*, 20246–20249.

Bhat, M.A., Izaddoost, S., Lu, Y., Cho, K.O., Choi, K.W., and Bellen, H.J. (1999). Discs Lost, a novel multi-PDZ domain protein, establishes and maintains epithelial polarity. Cell *96*, 833–845.

Bloor, J.W., and Kiehart, D.P. (2001). Zipper nonmuscle myosin-II functions downstream of PS2 integrin in *Drosophila* myogenesis and is necessary for myofibril formation. Dev. Biol. *239*, 215–228.

Bresnick, A.R. (1999). Molecular mechanisms of nonmuscle myosin-II regulation. Curr. Opin. Cell Biol. *11*, 26–33.

Bretscher, A. (1999). Regulation of cortical structure by the ezrin-radixin-moesin protein family. Curr. Opin. Cell Biol. *11*, 109–116.

Bridgman, P.C., Dave, S., Asnes, C.F., Tullio, A.N., and Adelstein, R.S. (2001). Myosin IIB is required for growth cone motility. J. Neurosci. *21*, 6159–6169.

Brown, J., and Bridgman, P.C. (2003a). Role of myosin II in axon outgrowth. J. Histochem. Cytochem. *51*, 421–428.

Brown, M.E., and Bridgman, P.C. (2003b). Retrograde flow rate is increased in growth cones from myosin IIB knockout mice. J. Cell Sci. *116*, 1087–1094.

Campos, A.R., Lee, K.J., and Steller, H. (1995). Establishment of neuronal connectivity during development of the *Drosophila* larval visual system. J. Neurobiol. *28*, 313–329.

Champagne, M.B., Edwards, K.A., Erickson, H.P., and Kiehart, D.P. (2000). *Drosophila* stretchin-MLCK is a novel member of the Titin/Myosin light chain kinase family. J. Mol. Biol. *300*, 759–777.

Chew, T.L., Masaracchia, R.A., Goeckeler, Z.M., and Wysolmerski, R.B. (1998). Phosphorylation of non-muscle myosin II regulatory light chain by p21-activated kinase (gamma-PAK). J. Muscle Res. Cell Motil. *19*, 839–854.

Craig, R., Smith, R., and Kendrick-Jones, J. (1983). Light-chain phosphorylation controls the conformation of vertebrate non-muscle and smooth muscle myosin molecules. Nature *302*, 436–439.

Crawford, J.M., Su, Z., Varlamova, O., Bresnick, A.R., and Kiehart, D.P. (2001). Role of myosin-II phosphorylation in V12Cdc42-mediated disruption of *Drosophila* cellularization. Eur. J. Cell Biol. *80*, 240–244.

Dahmann, C., and Basler, K. (1999). Compartment boundaries: at the edge of development. Trends Genet. *15*, 320–326.

Dent, E.W., and Gertler, F.B. (2003). Cytoskeletal dynamics and transport in growth cone motility and axon guidance. Neuron *40*, 209–227.

Edwards, K.A., and Kiehart, D.P. (1996). *Drosophila* nonmuscle myosin II has multiple essential roles in imaginal disc and egg chamber morphogenesis. Development *122*, 1499–1511.

Eto, M., Wong, L., Yazawa, M., and Brautigan, D.L. (2000). Inhibition of myosin/moesin phosphatase by expression of the phosphoinhibitor protein CPI-17 alters microfilament organization and retards cell spreading. Cell Motil. Cytoskeleton *46*, 222–234.

Fan, S.-S., and Ready, D.F. (1997). *Glued* participates in distinct microtubule-based activities in *Drosophila* eye development. Development *124*, 1497–1507.

Feng, J., Ito, M., Ichikawa, K., Isaka, N., Nishikawa, M., Hartshorne, D.J., and Nakano, T. (1999). Inhibitory phosphorylation site for Rho-associated kinase on smooth muscle myosin phosphatase. J. Biol. Chem. *274*, 37385–37390.

Fujioka, M., *et al*. (1998).. A new isoform of human myosin phosphatase targeting/regulatory subunit (MYPT2): cDNA cloning, tissue expression, and chromosomal mapping. Genomics *49*, 59–68.

Fukata, Y., Kimura, K., Oshiro, N., Saya, H., Matsuura, Y., and Kaibuchi, K. (1998). Association of the myosin-binding subunit of myosin phosphatase and moesin: dual regulation of moesin phosphorylation by Rho-associated kinase and myosin phosphatase. J. Cell Biol. *141*, 409–418.

Halsell, S.R., Chu, B.I., and Kiehart, D.P. (2000). Genetic analysis demonstrates a direct link between Rho signaling and nonmuscle myosin function during *Drosophila* morphogenesis. Genetics *156*, 469.

Hartshorne, D.J., Ito, M., and Erdodi, F. (1998). Myosin light chain phosphatase: subunit composition, interactions and regulation. J. Muscle Res. Cell Motil. *19*, 325–341.

Hing, H., Xiao, J., Harden, N., Lim, L., and Zipursky, S.L. (1999). Pak functions downstream of dock to regulate photoreceptor axon guidance in *Drosophila.* Cell *97*, 853–863.

Ikebe, M., Hartshorne, D.J., and Elzinga, M. (1986). Identification, phosphorylation, and dephosphorylation of a second site for myosin light chain kinase on the 20,000-dalton light chain of smooth muscle myosin. J. Biol. Chem. *261*, 36–39.

Jacinto, A., Wood, W., Woolner, S., Hiley, C., Turner, L., Wilson, C., Martinez-Arias, A., and Martin, P. (2002). Dynamic analysis of actin cable function during *Drosophila* dorsal closure. Curr. Biol. *12*, 1245–1250.

Jamora, C., and Fuchs, E. (2002). Intercellular adhesion, signalling and the cytoskeleton. Nat. Cell Biol. *4*, E101–E108.

Jankovics, F., Sinka, R., Lukacsovich, T., and Erdelyi, M. (2002). MOESIN crosslinks actin and cell membrane in *Drosophila* oocytes and is required for OSKAR anchoring. Curr. Biol. *12*, 2060–2065.

Janody, F., Lee, J.D., Jahren, N., Hazelett, D.J., Benlali, A., Miura, G.I., Draskovic, I., and Treisman, J.E. (2004). A mosaic genetic screen reveals distinct roles for *Polycomb* and *trithorax* group genes in *Drosophila* eye development. Genetics *166*, 187–200.

Jarman, A.P., Grell, E.H., Ackerman, L., Jan, L.Y., and Jan, Y.N. (1994). *atonal* is the proneural gene for *Drosophila* photoreceptors. Nature *369*, 398–400.

Jordan, P., and Karess, R. (1997). Myosin light chain-activating phosphorylation sites are required for oogenesis in *Drosophila.* J. Cell Biol. *139*, 1805–1819.

Karess, R.E., Chang, X.J., Edwards, K.A., Kulkarni, S., Aguilera, I., and Kiehart, D.P. (1991). The regulatory light chain of nonmuscle myosin is encoded by *spaghetti-squash*, a gene required for cytokinesis in *Drosophila.* Cell *65*, 1177–1189.

Katoh, K., Kano, Y., Amano, M., Onishi, H., Kaibuchi, K., and Fujiwara, K. (2001). Rho-kinase-mediated contraction of isolated stress fibers. J. Cell Biol. *153*, 569–584.

Kawano, Y., Fukata, Y., Oshiro, N., Amano, M., Nakamura, T., Ito, M., Matsumura, F., Inagaki, M., and Kaibuchi, K. (1999). Phosphorylation of myosin-binding subunit (MBS) of myosin phosphatase by Rho-kinase in vivo. J. Cell Biol. *147*, 1023–1038.

Kim, Y.S., Furman, S., Sink, H., and VanBerkum, M.F. (2001). Calmodulin and profilin coregulate axon outgrowth in *Drosophila.* J. Neurobiol. *47*, 26–38.

Kiosses, W.B., Daniels, R.H., Otey, C., Bokoch, G.M., and Schwartz, M.A. (1999). A role for p21-activated kinase in endothelial cell migration. J. Cell Biol. *147*, 831–844.

Kolega, J. (2003). Asymmetric distribution of myosin IIB in migrating endothelial cells is regulated by a rho-dependent kinase and contributes to tail retraction. Mol. Biol. Cell *14*, 4745–4757.

Korn, E.D. and Hammer, J.A. 3rd. (1988). Myosins of nonmuscle cells. Annu. Rev. Biophys. Biophys. Chem. *17*, 23–45.

Lee, S., and Kolodziej, P.A. (2002). Short Stop provides an essential link between F-actin and microtubules during axon extension. Development *129*, 1195–1204.

Lee, T., and Luo, L. (1999). Mosaic analysis with a repressible cell marker for studies of gene function in neuronal morphogenesis. Neuron *22*, 451–461.

Maciver, S.K. (1996). Myosin II function in non-muscle cells. Bioessays *18*, 179–182.

Matsui, T., Maeda, M., Doi, Y., Yonemura, S., Amano, M., Kaibuchi, K., and Tsukita, S. (1998). Rho-kinase phosphorylates COOH-terminal threonines of ezrin/radixin/moesin (ERM) proteins and regulates their head-to-tail association. J. Cell Biol. *140*, 647–657.

Matsui, T., Yonemura, S., and Tsukita, S. (1999). Activation of ERM proteins in vivo by Rho involves phosphatidyl-inositol 4-phosphate 5-kinase and not ROCK kinases. Curr. Biol. *9*, 1259–1262.

Maurel-Zaffran, C., and Treisman, J.E. (2000). *pannier* acts upstream of *wingless* to direct dorsal eye disc development in *Drosophila.* Development *127*, 1007–1016.

Mizuno, T., Amano, M., Kaibuchi, K., and Nishida, Y. (1999). Identification and characterization of *Drosophila* homolog of Rho-kinase. Gene *238*, 437–444.

Mizuno, T., Tsutsui, K., and Nishida, Y. (2002). *Drosophila* myosin phosphatase and its role in dorsal closure. Development *129*, 1215–1223.

Mosley-Bishop, K.L., Li, Q., Patterson, L., and Fischer, J.A. (1999). Molecular analysis of the *klarsicht* gene and its role in nuclear migration within differentiating cells of the *Drosophila* eye. Curr. Biol. *9*, 1211–1220.

Muller, H.A. (2003). Epithelial polarity in flies: more than just crumbs. Dev. Cell *4*, 1–3.

Ng, M., Diaz-Benjumea, F.J., and Cohen, S.M. (1995). *nubbin* encodes a POU-domain protein required for proximal-distal patterning in the *Drosophila* wing. Development *121*, 589–599.

Oda, H., Uemura, T., Harada, Y., Iwai, Y., and Takeichi, M. (1994). A *Drosophila* homolog of cadherin associated with armadillo and essential for embryonic cell-cell adhesion. Dev. Biol. *165*, 716–726.

Pearson, M.A., Reczek, D., Bretscher, A., and Karplus, P.A. (2000). Structure of the ERM protein moesin reveals the FERM domain fold masked by an extended actin binding tail domain. Cell *101*, 259–270.

Pearson, R.B., Jakes, R., John, M., Kendrick-Jones, J., and Kemp, B.E. (1984). Phosphorylation site sequence of smooth muscle myosin light chain (Mr = 20 000). FEBS Lett. *168*, 108–112.

Pellikka, M., Tanentzapf, G., Pinto, M., Smith, C., McGlade, C.J., Ready, D.F., and Tepass, U. (2002). Crumbs, the *Drosophila* homologue of human CRB1/RP12, is essential for photoreceptor morphogenesis. Nature *416*, 143–149.

Piekny, A.J., Wissmann, A., and Mains, P.E. (2000). Embryonic morphogenesis in *Caenorhabditis elegans* integrates the activity of LET-502 Rho-binding kinase, MEL-11 myosin phosphatase, DAF-2 insulin receptor and FEM-2 PP2c phosphatase. Genetics *156*, 1671–1689.

Pielage, J., Stork, T., Bunse, I., and Klambt, C. (2003). The *Drosophila* cell survival gene *discs lost* encodes a cytoplasmic Codanin-1-like protein, not a homolog of tight junction PDZ protein Patj. Dev. Cell *5*, 841–851.

Polesello, C., Delon, I., Valenti, P., Ferrer, P., and Payre, F. (2002). Dmoesin controls actin-based cell shape and polarity during *Drosophila melanogaster* oogenesis. Nat. Cell Biol. *4*, 782–789.

Ready, D.F., Hanson, T.E., and Benzer, S. (1976). Development of the *Drosophila* retina, a neurocrystalline lattice. Dev. Biol. *53*, 217–240.

Ridley, A.J., Schwartz, M.A., Burridge, K., Firtel, R.A., Ginsberg, M.H., Borisy, G., Parsons, J.T., and Horwitz, A.R. (2003). Cell migration: integrating signals from front to back. Science *302*, 1704–1709.

Rochlin, M.W., Itoh, K., Adelstein, R.S., and Bridgman, P.C. (1995). Localization of myosin II A and B isoforms in cultured neurons. J. Cell Sci. *108*, 3661–3670.

Schneeberger, D., and Raabe, T. (2003). Mbt, a *Drosophila* PAK protein, combines with Cdc42 to regulate photoreceptor cell morphogenesis. Development *130*, 427–437.

Shimizu, H., *et al*. (1994). Characterization of the myosin-binding subunit of smooth muscle myosin phosphatase. J. Biol. Chem. *269*, 30407–30411.

Speck, O., Hughes, S.C., Noren, N.K., Kulikauskas, R.M., and Fehon, R.G. (2003). Moesin functions antagonistically to the Rho pathway to maintain epithelial integrity. Nature *421*, 83–87.

Steller, H., Fischbach, K.F., and Rubin, G.M. (1987). *disconnected*: a locus required for neuronal pathway formation in the visual system of *Drosophila*. Cell *50*, 1139–1153.

Tan, C., Stronach, B., and Perrimon, N. (2003). Roles of myosin phosphatase during *Drosophila* development. Development *130*, 671–681.

Tanaka, J., Ito, M., Feng, J., Ichikawa, K., Hamaguchi, T., Nakamura, M., Hartshorne, D.J., and Nakano, T. (1998). Interaction of myosin phosphatase target subunit 1 with the catalytic subunit of type 1 protein phosphatase. Biochemistry *37*, 1697–1703.

Totsukawa, G., Yamakita, Y., Yamashiro, S., Hartshorne, D.J., Sasaki, Y., and Matsumura, F. (2000). Distinct roles of ROCK (Rho-kinase) and MLCK in spatial regulation of MLC phosphorylation for assembly of stress fibers and focal adhesions in 3T3 fibroblasts. J. Cell Biol. *150*, 797–806.

Uchida, K.S.K., Kitanishi-Yumura, T., and Yumura, S. (2003). Myosin II contributes to the posterior retraction and the anterior extension during the retraction phase in migrating *Dictyostelium* cells. J. Cell Sci. *116*, 51–60.

Umemoto, S., Bengur, A.R., and Sellers, J.R. (1989). Effect of multiple phosphorylations of smooth muscle and cytoplasmic myosins on movement in an in vitro motility assay. J. Biol. Chem. *264*, 1431–1436.

Vermeren, M., Maro, G.S., Bron, R., McGonnell, I.M., Charnay, P., Topilko, P., and Cohen, J. (2003). Integrity of developing spinal motor columns is regulated by neural crest derivatives at motor exit points. Neuron *37*, 403–415.

Wheatley, S., Kulkarni, S., and Karess, R. (1995). *Drosophila* nonmuscle myosin II is required for rapid cytoplasmic transport during oogenesis and for axial nuclear migration in early embryos. Development *121*, 1937–1946.

Winter, C.G., Wang, B., Ballew, A., Royou, A., Karess, R., Axelrod, J.D., and Luo, L. (2001). *Drosophila* Rho-associated kinase (Drok) links Frizzled-mediated planar cell polarity signaling to the actin cytoskeleton. Cell *105*, 81–91.

Wissmann, A., Ingles, J., and Mains, P.E. (1999). The *Caenorhabditis elegans mel-11* myosin phosphatase regulatory subunit affects tissue contraction in the somatic gonad and the embryonic epidermis and genetically interacts with the Rac signaling pathway. Dev. Biol. *209*, 111–127.

Wolff, T., Martin, K.A., Rubin, G.M., and Zipursky, S.L. (1997). The development of the *Drosophila* visual system. *In* Molecular and Cellular Approaches to Neural Development, ed. W.M. Cowan, T.M. Jessell, and S.L. Zipursky, Oxford, United Kingdom: Oxford University Press, 474–508.

Wylie, S.R., and Chantler, P.D. (2001). Separate but linked functions of conventional myosins modulate adhesion and neurite outgrowth. Nat. Cell Biol. *3*, 88–92.

Wylie, S.R., Wu, P.J., Patel, H., and Chantler, P.D. (1998). A conventional myosin motor drives neurite outgrowth. Proc. Natl. Acad. Sci. USA *95*, 12967–12972.

Young, P.E., Richman, A.M., Ketchum, A.S., and Kiehart, D.P. (1993). Morphogenesis in *Drosophila* requires nonmuscle myosin heavy chain function. Genes Dev. *7*, 29–41.

Zhao, D.B., Cote, S., Jahnig, F., Haller, J., and Jackle, H. (1988). *zipper* encodes a putative integral membrane protein required for normal axon patterning during *Drosophila* neurogenesis. EMBO J. *7*, 1115–1119.